Negative index media in microwave waveguide

Patanjali V. Parimi, Plarenta Vodo, and Srinivas Sridhar[a]
Department of Physics, Northeastern University 360 Huntington Avenue,
Boston, MA 02115,

John S. Derov and Beverly Turchinetz
AFRL/SNHA, 80 Scott Drive, Hanscom AFB, MA 01731.

Microwave waveguide measurements of negative index media (NIM) are reported. Accurate determination of the frequency variation of the complex scattering parameters yields the refractive index $\tilde{n}(\omega) = n'+in''$ for the NIM with n' varying between -3.9 to -0.3 in the passband region of 9.7-10.5 GHz. The results show that transmission is optimized for $n' \approx -1$ and small n''.
PACS numbers: 78.20.Ci, 42.25.Bs, 41.20.Jb, 42.70.Qs

The intriguing physical properties of metamaterial with negative refractive index, such as the anti-parallelism of the phase velocity and Poynting vector,[1] negative refraction,[2] and the amplification of evanescent waves,[3] can be exploited for several interesting technological applications. At microwave frequencies potential applications are in bandpass filters, beam steerers, microwave couplers and superlenses.

Negative refraction in NIM was demonstrated experimentally in parallel plate[2] and free space microwave measurements,[4] and there have been some theoretical investigations,[5,6] and experiments on related plasmonic materials.[7] Although negative refraction clearly indicates that the real part n' of the complex refractive index $\tilde{n}(\omega) = n'+in''$ is < 0 and leads to the determination of $n'(\omega)$, it is not easily used to determine the imaginary part $n''(\omega)$ which describes the absorptive losses. For technological applications, investigation of the dependence of transmission properties on various structural parameters and an accurate determination of the material parameters such as permittivity $\tilde{\varepsilon}(\omega) = \varepsilon'+i\varepsilon''$, permeability $\tilde{\mu}(\omega) = \mu'+i\mu''$ and especially $\tilde{n}(\omega)$ are vital, since one of the most interesting potential uses of the NIM, the superlens[3] (with perfect focusing through a parallel-sided slab) is possible only when $n' = -1$ and in the absence of losses, $n''= 0$.

One of the most sensitive and accurate methods to determine the aforementioned material parameters utilizes transmission in a waveguide partially filled with the material. This method is based on determining the propagation constant of the material from the guide scattering $\tilde{S}$parameters. It is essential in these measurements to accurately de-embed the sample data from other extraneous contributions. This procedure requires careful calibration that is best carried out in waveguide structures. The use of a highly sensitive vector network analyzer to obtain scattering parameters, the ease of accurate calibration and de-embedding, and high sensitivity due to large perturbation to the TE_{10} mode in the waveguide, result in a precise measurement of propagation constant and make this technique highly attractive. In this Letter we describe quantitative measurements of the material parameters of a structure designed to have negative index of refraction in the X-band.

Printed circuit board was etched using lithography techniques to produce arrays of split ring resonators (SRR) on
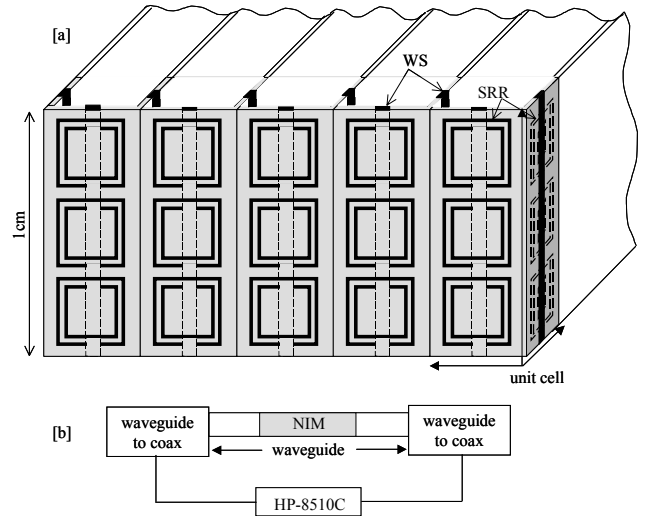

FIG. 1 Schematic diagram of NIM (a) and S-parameter measurement set up (b). In (a), SRR and WS are shown with solid and dashed lines exemplifying them on both sides of the substrate. Each unit cell has dimensions 1 x 0.5 x 0.5 cm^3.

[a] Email: s.sridhar@neu.edu

one side and wire strips (WS) on the other side of the board. An array of SRR and WS should result in an effective negative permeability and negative permittivity material. Therefore a lattice of material was assembled with unit cell consisting of two sets paired at right angles of three SRR and one WS each, as illustrated in Fig. 1a, to produce a material that notionally has $n' < 0$ [8]. The thickness of the WS is 30 μm and width is 1mm. Each SRR has two rings of thickness 30 μm with the larger ring having each side 2.6 mm. Two different substrate materials, Taconic FR-35 and commercial G10, both with $\varepsilon' = 4.7$ in the microwave region, were used to fabricate two NIMs, M1 and M2, respectively. M1 was assembled by interleaving the circuit board strips parallel to one another in the z direction unlike M2 which was assembled by interleaving circuit board strips in both x and z directions, as shown in Fig. 1a.

The NIM of interest is inserted in a rectangular X-band waveguide with cross section 2.286 x 1.0 cm^2 such that the WS are parallel to the short dimension (y direction) of the waveguide, as illustrated in Fig. 1b. The length of the waveguide is 9.3 cm. All four complex S-parameters are measured using an HP8510C vector network analyzer between 8 and 12 GHz for which the empty waveguide propagates in the TE$_{10}$ mode. A through-reflect-line calibration was used to de-embed the S-parameters ($\widetilde{S}_{11}$, $\widetilde{S}_{21}$) of the waveguide sample holder, from which the S-parameters of the sample section of length d (5 cm) were extracted.

The waveguide transmission measurements were carefully performed first with both ends of the WS of the NIM connected to the top and bottom walls of the waveguide in the y direction with a thin copper tape and silver paint ensuring electrical continuity, and also without connecting the WS. As discussed later the former ensures a wider region of negative permittivity.
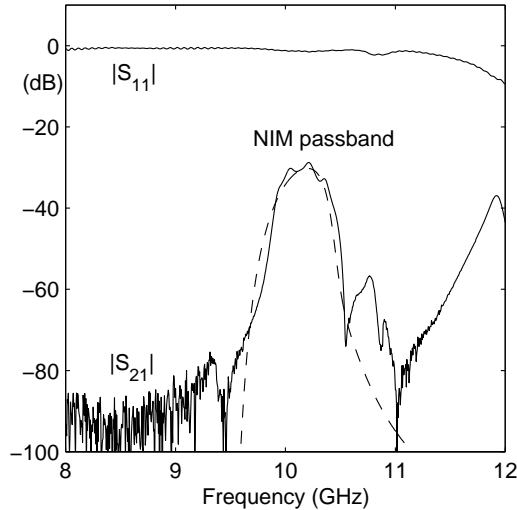

FIG.2 Magnitude of the transmission |S$_{21}$| and reflection |S$_{11}$| coefficients as a function of frequency for M1 measured in a waveguide. Solid lines represent the measured data and the dashed line is a fit to the theoretical model.

Fig. 2 shows the magnitude of the transmission $|S_{21}|$ and reflection $|S_{11}|$ coefficients of the material M1 when the WS are connected. A broad passband with a peak at -29 dB between 9.7 - 10.5 GHz is clearly evident in the $|S_{21}|$ response. The passband is bracketed by low transmittance regions, and is attributed to $n' < 0$ as discussed below. Another passband starting at 11.2 GHz can also be observed.
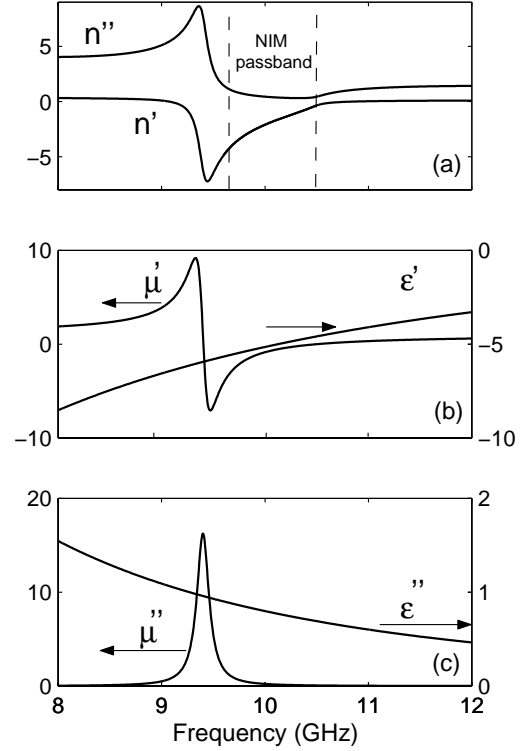

FIG.3 Real and imaginary parts of the complex $\widetilde{n}(\omega)$, $\widetilde{\varepsilon}(\omega)$ and $\widetilde{\mu}(\omega)$ determined from the theoretical fit to the measured data. $\widetilde{n}(\omega)$ varies from –3.9 to –0.3 in the region 9.7 - 10.5 GHz.

Introducing the reflection coefficient between a medium and the vacuum, $\Gamma = (\mu k_z - k_{rz})/(\mu k_z + k_{rz})$, the reflection and transmission S-parameters of the electromagnetic wave through a slab of material inside a waveguide can be shown to be[9]

$$S_{11} = \frac{(1 - e^{2ik_{rz}d})\Gamma}{1 - \Gamma^2 e^{2ik_{rz}d}}, \quad S_{21} = \frac{(1 - \Gamma^2)e^{ik_{rz}d}}{1 - \Gamma^2 e^{2ik_{rz}d}} \quad (1)$$

where $k_{rz} = \pm\sqrt{k^2 - k_x^2}$ with $k = n(\omega)\omega/c$ and $k_x = \pi/a$, is the z-component of the wave vector inside the waveguide. Analytic calculations suggest that effective $\widetilde{\mu}(\omega)$ of SRR[10] and $\widetilde{\varepsilon}(\omega)$ of WS[11] can be described by

$$\widetilde{\mu}(\omega) = 1 - \frac{\omega_{mp}^2 - \omega_{m0}^2}{\omega^2 - \omega_{m0}^2 + i\gamma_m\omega} \quad (2)$$

$$\widetilde{\varepsilon}(\omega) = 1 - \frac{\omega_{ep}^2 - \omega_{e0}^2}{\omega^2 - \omega_{e0}^2 + i\gamma_e\omega} \quad (3)$$

2

where ω_{eo} and ω_{mo} are low frequency edges of the electric and magnetic forbidden bands, ω_{ep} and ω_{mp} are electric and magnetic plasma frequencies, and γ_e and γ_m are the corresponding damping factors. The refractive index $\tilde{n}(\omega) = \pm\sqrt{\tilde{\varepsilon}(\omega)\tilde{\mu}(\omega)}$ has $n' < 0$ in the range $\max(\omega_{mo}, \omega_{eo}) < \omega < \min(\omega_{mp}, \omega_{ep})$.

Good agreement of the model to the measured $|S_{21}|$ of M1, as shown in Fig. 2, results from the fit parameters $f_{e0}=0$ GHz, $f_{ep}=25$ GHz, $f_{m0}=9.4$ GHz, $f_{mp}=10.5$ GHz, $\gamma_e= 1.3$ GHz and $\gamma_m=143$MHz (note $f=\omega/2\pi$). The measured data deviates from the model above 10.6 GHz due to the resonance driven by the proximity of the NIM elements to the walls of the waveguide and secondly due to the onset of a higher order mode above 11.2 GHz.

In Fig. 3 we show the real and imaginary parts of $\tilde{n}(\omega)$, $\tilde{\varepsilon}(\omega)$ and $\tilde{\mu}(\omega)$ obtained using the above fit parameters. It is important to note from Fig. 3a that the NIM is associated with $n' < 0$ and that in this region $n'(\omega)$ varies between -0.3 to -3.9. The NIM passband occurs in the region, 9.7 - 10.5 GHz that is also characterized by small n'' (Fig. 2a). Thus on the low frequency side even though both $\mu'(\omega) < 0$ and $\varepsilon'(\omega) < 0$ and hence $n'(\omega) < 0$ between 9.4 and 9.7 GHz (Fig. 2b), the transmission is highly attenuated because of the resonant nature due to which n'' is large. It can be observed from Figs. 2 and 3a that the transmission is maximum at 10.2 GHz where $n' \approx -1$, consistent with expectations.
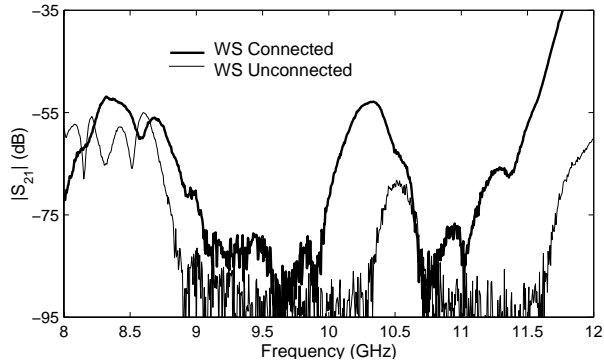

FIG.4 Magnitude of the transmission coefficient |S21| as a function of frequency for well-connected and unconnected wire strips of M2. Note the transmission enhancement for the well-connected strips.

The difference in the magnitude of $|S_{21}|$ for well-connected and unconnected WS of the material W2 is shown in Fig. 4. In both cases a passband can be seen around 10 GHz. It is interesting to observe that higher power is transmitted and the passband is broader in the connected case. The discontinuity in the unconnected WS results in a capacitance between the WS and the walls of the waveguide, and changes f_{e0} and f_{ep} (Eqn. 3), thereby reducing the region of negative permittivity. The effect of this on f_{e0} can be clearly observed from Fig. 4 since the lower edge of the NIM passband moved up to 10.3 GHz when the WS were unconnected. However, the higher edge of the passband at 10.7 GHz is not affected in either case. These observations validate the present description of f_{e0}. We believe that the lower edge of the passband at 9.9 GHz is due to f_{m0}.

In Fig. 4 an additional lower frequency passband between 8 and 9 GHz in M2 can be observed. From the model analysis this passband is because f_{eo} is pushed up to around 8 GHz for this structure. While we have presented data from two metamaterials that represent typical NIM characteristics, we have actually measured transmission characteristics of several NIM. In some cases we have observed much lower attenuation about –18 dB. This suggests that the NIM and PIM passbands can be tailored by changing the design parameters and substrate material. The measured transmission of M1 with Taconic FR-35 substrate (Fig. 2) differs from that of M2 with G10 (Fig. 4). The high losses in M2 with the passband peak at -52 dB as against the passband peak at -29dB for M1 suggest that the substrate material plays an important role in determining the transmission characteristics.

In conclusion, waveguide transmission measurements on the NIM yield quantitative information on the metamaterial properties. The index of refraction $n'(\omega)$ determined from the theoretical fit of the model expression to the measured data is found to vary from -3.9 to -0.3 in the passband region 9.7 to 10.5 GHz. The results show that transmission is optimized for $n' \sim -1$ and low n''. It appears best to operate away from the resonant frequency of the material to achieve these conditions. The results suggest that substantial improvements in performance are feasible by reducing n'' significantly through better design with low loss substrates and ensuring continuity of the WS to broaden the NIM region.

[1] V. G. Veselago, Sov. Phys. USPEKHI **10**, 509 (1968).

[2] R. A. Shelby, D. R. Smith, and S. Schultz , Science **292**, 77 (2001).

[3] J. B. Pendry, Phys. Rev. Lett **85**, 3966 (2000).

[4] C. G. Parazzoli , R. B. Greegor, and K. Li, Preprint **0**, 0 (2002).

[5] D. R. Smith, S. Schultz, P. Markos , and C. M. Soukoulis, Phys. Rev B **65**, 195104-1 (2002).

[6] Jin Au Kong, Bae-lan Wu, and Yan Zhang, Appl. Phys. Lett **80**, 2084 (2002).

[7] P. Gay-Balmaz, C. Maccio, and O. J. F. Martin, Appl. Phys. Lett **81**, 2896 (2002).

[8] R. A. Shelby, D. R. Smith, S. C. Nemat-Nasser, and S. Schultz , Appl. Phys. Lett **78**, 489 (2001).

[9] A. M. Nicolson and G. F. Ross, IEEE Trans. Instrum. Meas. **19**, 377 (1970).

[10] J. B. Pendry, A. Holden, D. J. Robbins, and W. Stewart, IEEE Trans. Microwave Theory and Techniques **47**, 2075 (1999).

[11] J. B. Pendry, A. J. Holden, W. Stewart, and I. Youngs, Phys. Rev. Lett **76**, 4733(1966).